Independent roles of Fgfr2 and Frs2α in ureteric epithelium

Sunder Sims-Lucas[1], Brian Cusack[1], Veraragavan P. Eswarakumar[2], Jue Zhang[3], Fen Wang[3] and Carlton M. Bates[1,4,*]

SUMMARY

Mice with conditional deletion of fibroblast growth factor receptor 2 (*Fgfr2*) in the ureteric bud using a *Hoxb7cre* line (*Fgfr2$^{UB-/-}$*) develop severe ureteric branching defects; however, ureteric deletion of fibroblast growth factor receptor substrate 2α (*Frs2α*), a key docking protein that transmits fibroblast growth factor receptor intracellular signaling (*Frs2α$^{UB-/-}$*) leads to mild ureteric defects. Mice with point mutations in the Frs2α binding site of Fgfr2 (*Fgfr2$^{LR/LR}$*) have normal kidneys. The aim of this study was to determine the relationship between Fgfr2 and Frs2α in the ureteric lineage. Mice with ureteric deletion of both *Fgfr2* and *Frs2α* (*Fgfr2/Frs2α$^{UB-/}$*) were compared with *Frs2α$^{UB-/-}$* and *Fgfr2$^{UB-/-}$* mice. To avoid potential rescue of Fgfr1 forming heterodimers with Fgfr2^{LR} alleles to recruit Frs2α, compound mutant mice were generated with ureteric deletion of *Fgfr1* and with *Fgfr2$^{LR/LR}$* point mutations (*Fgfr1$^{UB-/-}$Fgfr2$^{LR/LR}$*). At E13.5, three-dimensional reconstructions and histological assessment showed that, whereas *Fgfr2$^{UB-/-}$* kidneys had more severe ureteric branching defects than *Frs2α$^{UB-/-}$*, *Fgfr2$^{UB-/-}$* kidneys were indistinguishable from *Fgfr2/Frs2α$^{UB-/-}$*. At later stages, however, *Fgfr2/Frs2α$^{UB-/-}$* kidneys were more severely affected than either *Fgfr2$^{UB-/-}$* or *Frs2α$^{UB-/-}$* kidneys. Taken together, although Fgfr2 and Frs2α have crucial roles in the ureteric lineage, they appear to act separately and additively.

KEY WORDS: Fibroblast growth factor receptor 2, Frs2α, Ureteric epithelium, Mouse

INTRODUCTION

Metanephric kidney development occurs via interactions of the ureteric bud (UB) and metanephric mesenchyme (MM) (Costantini and Kopan, 2010). The UB grows out from the Wolffian duct, receiving signals from the adjacent MM. The UB then elongates, contacts the MM and then branches within the MM over several generations. Terminal UB tips induce surrounding MM-derived nephron progenitors to condense and then differentiate into epithelial nephrons. Cortical stromal mesenchyme also forms and ultimately differentiates into interstitial cells.

Fibroblast growth factor receptor (Fgfr) signaling is crucial for kidney development. Fgfrs are receptor tyrosine kinases (RTKs) with four signaling family members and 22 known mammalian ligands (Powers et al., 2000). Many investigators have shown that Fgf ligands and receptors have crucial roles in renal mesenchymal and ureteric lineages, often with conditional knockout approaches (Barasch et al., 1997; Barasch et al., 1999; Celli et al., 1998; Hains et al., 2008; Li et al., 2006; Nguyen et al., 1996; Ohuchi et al., 2000; Perantoni et al., 1995; Poladia et al., 2006; Qiao et al., 2001; Qiao et al., 1999; Revest et al., 2001; Zhao et al., 2004). We demonstrated that conditional deletion of *Fgfr2* using a *Hoxb7cre* line (targeting the UB) results in aberrant ureteric and cortical stromal patterning (Zhao et al., 2004).

Fgfr signaling is mediated via docking adapter proteins that transmit intracellular signaling. One well-characterized adapter is fibroblast growth factor receptor substrate 2α (Frs2α; Frs2 – Mouse Genome Informatics) (Gotoh, 2008). Frs2α binds constitutively in the receptor juxtamembrane region and upon Fgfr simulation becomes phosphorylated, ultimately activating Erk, Akt and protein kinase C (PKC) λ and ξ. Frs2α also serves as an adapter protein for other RTKs such as neurotrophin receptors and Ret (Gotoh, 2008). Global deletion of *Frs2α* results in early embryonic lethality, presumably due to the inability of some RTKs to signal properly (Hadari et al., 2001).

Given that Frs2α is utilized by Fgfr2 and Ret, both of which are crucial for ureteric morphogenesis (Schuchardt et al., 1994; Zhao et al., 2004), we investigated the role of Frs2α in the UB by conditional deletion with our *Hoxb7cre* line (Sims-Lucas et al., 2009b). Inactivation of Frs2α in ureteric tissues resulted in mild renal hypoplasia with slightly fewer ureteric tips and normal stromal patterning. Furthermore, mice with point mutations in Fgfr2 that replace amino acids Leu-424 (L) and amino acid Arg-426 (R) with Ala residues (*Fgfr2$^{LR/LR}$*) to prevent Frs2α binding to the receptor had normal kidneys (Eswarakumar et al., 2006; Sims-Lucas et al., 2009b).

To understand the relationship between Fgfr2 and Frs2α in the UB, we examined mice with combined conditional deletion of *Fgfr2* and *Frs2α* with our *Hox7bcre* line (*Fgfr2/Frs2α$^{UB-/-}$*) in comparison with deletion of *Frs2α* alone (*Frs2α$^{UB-/-}$*) or *Fgfr2* alone (*Fgfr2$^{UB-/-}$*). To avoid potential rescue of intact Fgfr1 forming heterodimers with Fgfr2^{LR} point mutants to recruit Frs2α, we generated mice with conditional deletion of *Fgfr1* from the UB and with the *Fgfr2$^{LR/LR}$* point mutations (*Fgfr1$^{UB-/-}$Fgfr2$^{LR/LR}$*). At E13.5, three-dimensional (3D) reconstructions and histological assessment confirmed that *Fgfr2$^{UB-/-}$* kidneys had more severe ureteric branching defects than *Frs2α$^{UB-/-}$*, but that *Fgfr2$^{UB-/-}$* kidneys were indistinguishable from *Fgfr2/Frs2α$^{UB-/-}$*. At

[1]Rangos Research Center, Children's Hospital of Pittsburgh of UPMC, Pittsburgh, PA 15201, USA. [2]Department of Orthopaedics and Rehabilitation, Yale University School of Medicine, New Haven, CT 06520, USA. [3]Center for Cancer Biology and Nutrition, Institute of Biosciences and Technology, Texas A&M, Houston, TX 77030, USA. [4]Division of Nephrology, Department of Pediatrics, University of Pittsburgh School of Medicine, Pittsburgh, PA 15201, USA.

*Author for correspondence (batescm@upmc.edu)

later stages, however, $Fgfr2/Frs2\alpha^{UB-/-}$ kidneys were more severely affected than $Fgfr2^{UB-/-}$ or $Frs2\alpha^{UB-/-}$ kidneys. $Fgfr1^{UB-/-}Fgfr2^{LR/LR}$ mice had phenotypically normal kidneys. Thus, although Fgfr2 and Frs2α each have crucial roles in the ureteric lineage, they appear to act independently and additively.

MATERIALS AND METHODS

Mouse strains

Our *Hoxb7cre* line has been shown to drive efficient deletion of *Fgfr1*, *Fgfr2* and *Frs2α* in the UB (Sims-Lucas et al., 2009b; Zhao et al., 2004). For this study, $Fgfr2^{Lox/Lox}$ [gift from Dr David Ornitz, Washington University, St Louis, MO, USA (Yu et al., 2003)] were bred with $Frs2\alpha^{Lox/Lox}$ mice (Lin et al., 2007) to produce $Fgfr2^{Lox/Lox}Frs2\alpha^{Lox/Lox}$ mice. These mice were bred with $Hoxb7creEGFP^{Tg/+}$ to generate $Hoxb7creEGFP^{Tg/+}Fgfr2^{Lox/+}Frs2\alpha^{Lox/+}$ mice. These mice were bred back with $Fgfr2^{Lox/Lox}Frs2\alpha^{Lox/Lox}$ to produce mice with ureteric epithelial deletion of $Frs2\alpha$ ($Frs2\alpha^{UB-/-}$), $Fgfr2$ ($Fgfr2^{UB-/-}$) or both ($Fgfr2/Frs2\alpha^{UB-/-}$) (see Table S1 in the supplementary material). We used similar breeding strategies to generate mice with ureteric deletion of *Fgfr1* ($Fgfr1^{UB-/-}$), with point mutations in the Frs2α binding site on Fgfr2 ($Fgfr2^{LR/LR}$), or both ($Fgfr1^{UB-/-}Fgfr2^{LR/LR}$) (see Table S2 in the supplementary material). When a vaginal plug was identified, noon of that day was deemed embryonic day 0.5 (E0.5).

Genotyping

Briefly, genomic DNA was isolated from tail clippings and/or embryonic tissues. Polymerase chain reaction (PCR) amplification identified the various alleles. For the *HoxCreEgfp* cassette, the forward primer 5′-AGCGCGATCACATGGTCCTG-3′ and reverse primer 5′-ACGATCCTGAGACTTCCACACT-3′ yielded a 230 base pair (bp) band identifying cre. For the *Frs2α* allele, the forward primer 5′-GAGTGTGCTGTGATTGGAAGGCAG-3′ and reverse primer 5′-GGCACGAGTGTCTGCAGACACATG-3′ yielded a 224 bp wild type and a 319 bp floxed band. For the *Fgfr2* allele, the forward primer 5′-GTCAATTCTAAGCCACTGTCTGCC-3′ and reverse primer 5′-CTCCACTGATTACATCTAAAGAGC-3′ yielded a 307 bp wild type and a 373 bp floxed band. For the $Fgfr2^{LR}$ allele, the forward primer 5′-GAGTACCATGCTGACTGCATGC-3′ and the reverse primer 5′-GGAGAGGCATCTCTGTTTCAAGACC-3′ yielded a 225 bp wild type and a 315 bp mutant band.

Histology

Embryos and/or kidneys were fixed in 4% paraformaldehyde (PFA) in phosphate buffered saline overnight at 4°C. Kidneys were examined under direct light and photographed with a fluorescence microscope to visualize the ureteric tree. Other tissues were placed in 70% ethanol at 4°C (for section histology) or dehydrated into 100% methanol at 4°C (for whole-mount histology). Tissues used for section histology were processed, embedded into paraffin and sectioned at 7 μm. Sections were stained with Hematoxylin and Eosin (H&E) or were subjected to non-radioactive in situ hybridization (ISH) for *Foxd1* as described (Zhao et al., 2004).

E17.5 kidneys were also subjected to whole-mount immunostaining with antibodies against monoclonal mouse anti-calbindin-D$_{28k}$ antisera (C9848, Sigma-Aldrich, MO, USA). Briefly, kidneys were rehydrated through methanol into PBST (PBS with 0.1% Tween 20) and blocked in 10% donkey serum. Tissues were incubated with primary antisera (1:100) overnight at 4°C. Kidneys were washed in PBST and incubated with Alexa Fluor 488 goat anti-mouse (1:100; A11001, Invitrogen, Carlsbad, CA, USA) overnight at 4°C. Kidneys were washed, mounted and imaged with an LSM 710 confocal microscope (Carl Zeiss MicroImaging, Thornwood, NY, USA).

E17.5 kidney sections were also subjected to aquaporin 2 (Aqp2) immunostaining. Control and $Fgfr2Frs2a^{UB-/-}$ ($n=3$ per genotype) paraffin kidney sections (4 μm) through renal papilla were de-waxed and hydrated. After permeabilizing with 0.1% Tween 20-PBS, tissues were blocked in 5% goat serum for 30 minutes. Sections were then incubated with polyclonal rabbit anti-Aqp2 (1:100; Calbiochem, CA, USA) for 45 minutes at 37°C. Kidneys were washed with PBS and then streptavidin-peroxidase staining was performed using an ABC kit (Vector Labs, CA, USA).

Glomerular profiling

P30 control, $Frs2a^{UB-/-}$, $Fgfr2^{UB-/-}$ and $Fgfr2Frs2a^{UB-/-}$ kidneys ($n=3$ per genotype) were bisected in the transverse plane, fixed in 4% PFA, processed to paraffin, and H&E stained. From the midline plane, three 4 μm sections were obtained at 200 μm intervals and every glomerulus per level was traced using Stereoinvestigator [Microbrightfield (MBF), VT, USA] to measure total and mean cross-sectional area and perimeter ($n=452$ for controls; $n=388$ for $Frs2a^{UB-/-}$; $n=335$ for $Fgfr2^{UB-/-}$; $n=153$ for $Fgfr2Frs2a^{UB-/-}$).

Morphometric measurements

E17.5 mutant and control embryos were sacrificed and weighed. Kidneys were removed, weighed and photographed. Cross-sectional area (area), and kidney long axis were measured using Image J analysis software (version 1.32j from Wayne Rasband, National Institutes of Health, USA).

3D rendering

3D reconstructions of E13.5 kidney capsules and ureteric trees were performed as described with slight modifications for skeletonizations (Sims-Lucas et al., 2009a). Briefly, image layers were generated from serial H&E stained sections by tracing capsules and ureteric tissues using Stereoinvestigator. Traced layers were aligned, rendering 3D images to show any traced structures. Using Neurolucida Explorer (MBF), volume and surface area were calculated for kidneys and the UB. From this, relative volumes and surface areas of ureteric epithelium (ureteric volume per kidney volume and ureteric surface area per kidney area) were determined. To skeletonize the ureteric tree, individual layers were exported into Microsoft Paint (Redmond, WA, USA) and tracings were filled in and saved as tiff files. Images were imported into Imaris software (Bitplane, Zurich, Switzerland) and a 3D skeleton of the ureteric tree was generated. Number of branch points and tips, lengths of branches (ureteric segments between two branch points), tips (ureteric segments from the last branch point to the outer cortex) and total ureteric segments (all segments including branches and tips) were calculated. Movies and still images of intact and skeletonized ureteric trees were generated.

Statistical analysis

Statistical analyses were performed using Student's *t*-test or one-way analysis of variance (ANOVA) followed by Student-Newman-Keuls post-hoc tests. Values are represented as mean ± standard deviation.
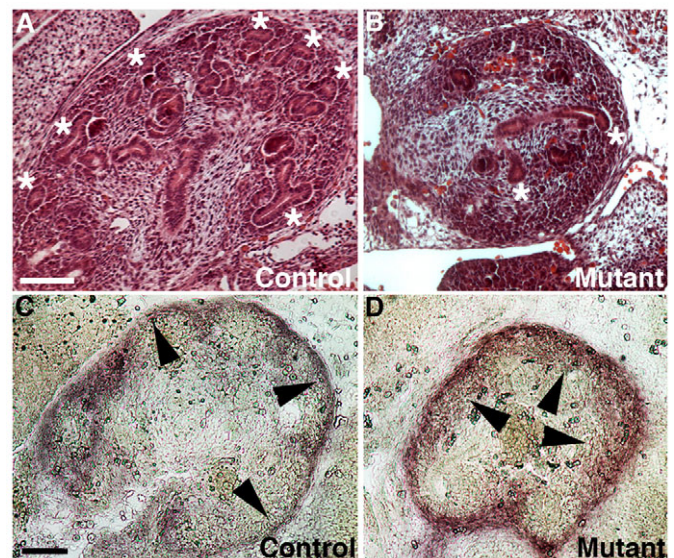

Fig. 1. Histological abnormalities in E13.5 $Fgfr2/Frs2\alpha^{UB-/-}$ kidneys. (**A**,**B**) H&E sections show that compared with controls (A), mutants (B) have fewer ureteric tips (asterisks) and developing nephrons. (**C**,**D**) *Foxd1* in situ hybridization shows that compared with cortical stroma in controls (C, arrowheads), mutants (D) have regions of aberrantly thickened cortical stroma (arrowheads). Scale bars: 100 μm.

RESULTS AND DISCUSSION
At E13.5, *Fgfr2*$^{UB-/-}$ kidneys had more severe defects than *Frs2*α$^{UB-/-}$, but *Fgfr2*$^{UB-/-}$ and *Fgfr2/Frs2*α$^{UB-/-}$ kidneys appear similar

Although *Frs2*α$^{UB-/-}$ mice in this study were also heterozygous for *Fgfr2*, we observed no obvious differences between these embryonic kidneys compared with previously published *Frs2*α$^{UB-/-}$ embryos that were wild type at the *Fgfr2* locus (Sims-Lucas et al., 2009b). Likewise, we observed no differences in *Fgfr2*$^{UB-/-}$ embryonic kidneys in this study (that were heterozygous for *Frs2*α) and kidneys from previously published *Fgfr2*$^{UB-/-}$ embryos (that were wild type for *Frs2*α) (Sims-Lucas et al., 2009a; Zhao et al., 2004).

Compared with controls, H&E sections of E13.5 *Fgfr2/Frs2*α$^{UB-/-}$ kidneys revealed dramatic decreases in ureteric branching, with large cortical regions devoid of ureteric tips, and with fewer developing nephrons (Fig. 1). *Foxd1* in situ hybridization revealed abnormal cortical stromal thickening in *Fgfr2/Frs2*α$^{UB-/-}$ kidneys compared with controls (Fig. 1). Thus, at E13.5, *Fgfr2/Frs2*α$^{UB-/-}$ mice had aberrant UB and cortical stromal development, appearing similar to *Fgfr2*$^{UB-/-}$ kidneys, but more severely affected than *Frs2*α$^{UB-/-}$ kidneys (Sims-Lucas et al., 2009b; Zhao et al., 2004).

To quantitate differences among mutants, we generated 3D reconstructions of E13.5 kidneys and ureteric trees. Mean kidney surface area, length and volume of *Fgfr2/Frs2*α$^{UB-/-}$ and *Fgfr2*$^{UB-/-}$ embryos were lower (or trended lower) than control and *Frs2*α$^{UB-/-}$ embryos (Fig. 2; see Fig. S1 and Table S3 in the supplementary material). *Fgfr2/Frs2*α$^{UB-/-}$ and *Fgfr2*$^{UB-/-}$ kidney sizes were not statistically different, however, as was the case between control and *Frs2*α$^{UB-/-}$ kidneys. 3D reconstructed ureteric trees showed that, compared with controls, *Frs2*α$^{UB-/-}$ kidneys had mild branching defects (fewer tips and branches and less ureteric tissue per kidney volume), whereas *Fgfr2/Frs2*α$^{UB-/-}$ and *Fgfr2*$^{UB-/-}$ had more severe defects (Fig. 2; see Movies 1-4 in the supplementary material). Compared with controls, mean ureteric volume and surface areas (absolute and relative) were modestly reduced in *Frs2*α$^{UB-/-}$ kidneys and more severely decreased in *Fgfr2/Frs2*α$^{UB-/-}$ and *Fgfr2*$^{UB-/-}$ (the latter two were not statistically different from each other) (Fig. 2; see Fig. S1 and Table S3 in the supplementary material). Images of skeletonized ureteric trees reinforced observations that, compared with controls, *Frs2*α$^{UB-/-}$ kidneys had moderate branching defects, but *Fgfr2/Frs2*α$^{UB-/-}$ and *Fgfr2*$^{UB-/-}$ had even more severe defects (Fig. 2; see Movies 5-8 in the supplementary material). Measurements of skeletonized trees confirmed that
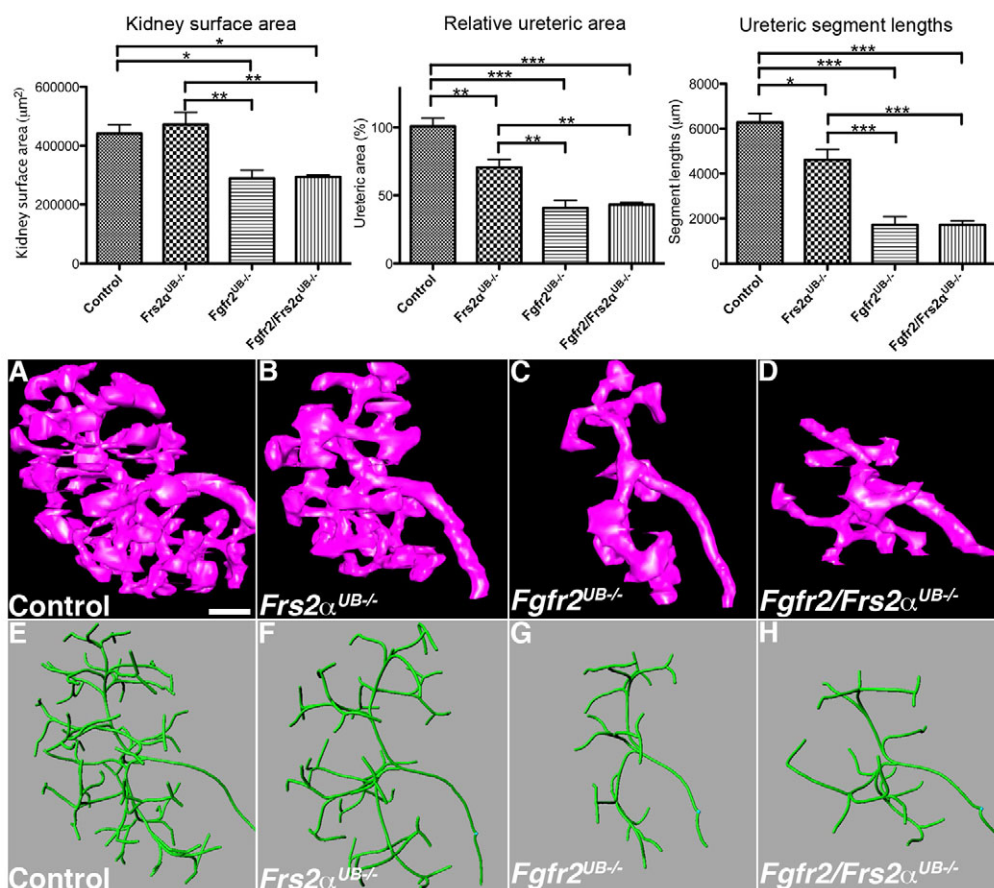

Fig. 2. 3D reconstructions in E13.5 *Fgfr2/Frs2*α$^{UB-/-}$, *Fgfr2* $^{UB-/-}$ and *Frs2*α$^{UB-/-}$ kidneys. Top left: Graph demonstrates that control (*n*=4) and *Frs2*α$^{UB-/-}$ (*n*=5) kidneys are larger than *Fgfr2*$^{UB-/-}$ (*n*=4) and *Fgfr2/Frs2*α$^{UB-/-}$ (*n*=3) kidneys and that the latter two are not statistically different from each other. Top middle and right: Graphs demonstrate that relative ureteric surface area and ureteric segment lengths are largest in controls followed by *Frs2*α$^{UB-/-}$, and then by *Fgfr2*$^{UB-/-}$ and *Fgfr2/Frs2*α$^{UB-/-}$. *$P<0.05$; **$P<0.01$; ***$P<0.001$. (**A-H**) Images of 3D reconstructions show that, compared with controls (A,E) (*n*=4), *Frs2*α$^{UB-/-}$ (B,F) (*n*=5) have moderate ureteric branching defects, including fewer tips and branches as well as proportionally less ureteric tissue per kidney volume. The branching defects are more severe in *Fgfr2*$^{UB-/-}$ (C,G) (*n*=4) and *Fgfr2/Frs2*α$^{UB-/-}$ (D,H) (*n*=3) mice. Scale bar: 100 μm.
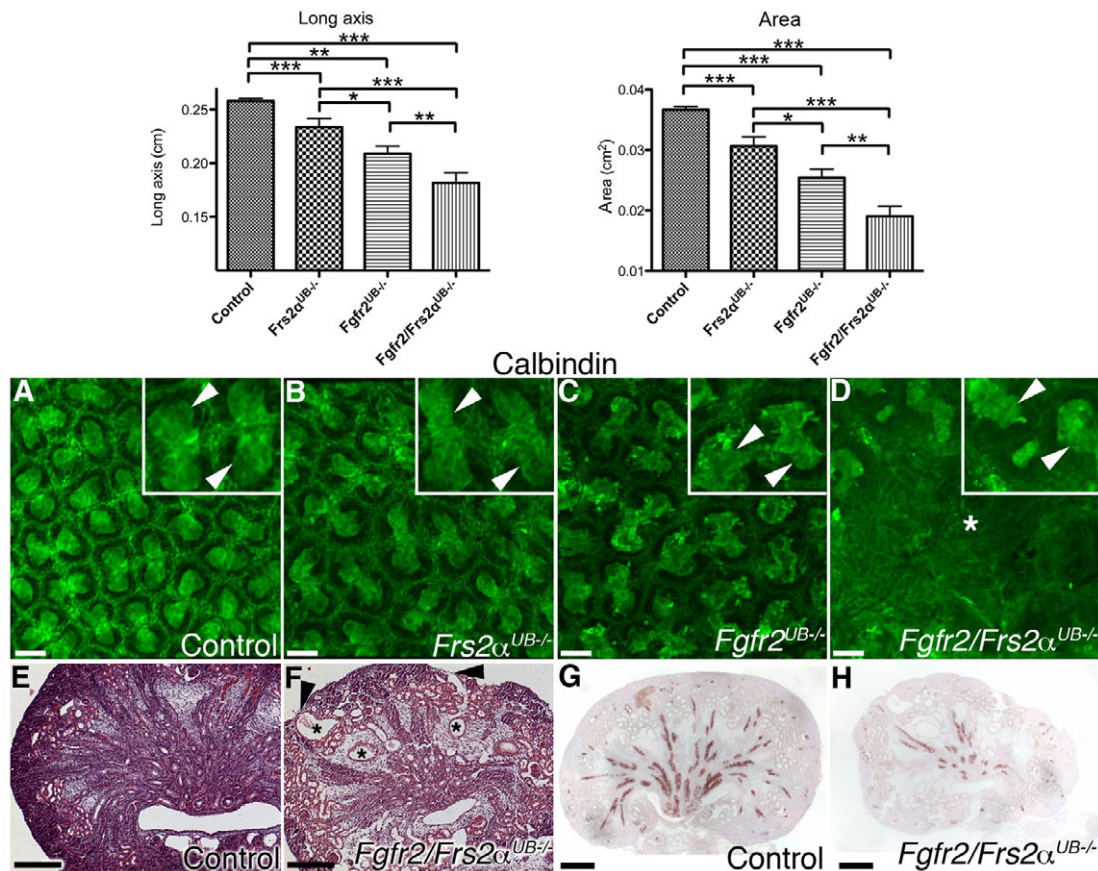
Fig. 3. E17.5 *Fgfr2/Frs2α^UB–/–*, *Fgfr2^UB–/–* and *Frs2α^UB–/–* kidneys. Top: Graphs demonstrate decreasing kidney long axis and cross-sectional area (area) from control to *Frs2α^UB–/–* to *Fgfr2^UB–/–* to *Fgfr2/Frs2α^UB–/–* mice. *$P<0.05$; **$P<0.01$; ***$P<0.001$. (**A-D**) Calbindin whole-mount immunofluorescence demonstrates worsening UB defects from control (A) to *Frs2α^UB–/–* (B) to *Fgfr2^UB–/–* (C) to *Fgfr2/Frs2α^UB–/–* mice (D), including wider spaces between tips, distorted tip shapes (arrowheads in upper right corners show 2× magnified tips), and large areas devoid of tips in *Fgfr2/Frs2α^UB–/–* kidneys (asterisk). (**E-H**) H&E stains show that, compared with controls (E), *Fgfr2/Frs2α^UB–/–* (F) have distorted renal architecture including thin renal cortex (arrowheads) overlying dilated tubules (asterisks). Aquaporin 2 immunostaining demonstrates that, compared with controls (G), *Fgfr2/Frs2α^UB–/–* mutants (H) have fewer collecting ducts. Scale bars: 100 μm for A-D; 250 μm for E-H.

mean total ureteric segment lengths and numbers (branches, tips and all segments) were greatest in controls, followed by *Frs2α^UB–/–*, and then *Fgfr2/Frs2α^UB–/–* and *Fgfr2^UB–/–* (the latter two were not statistically different from each other) (Fig. 2 and see Table S3 in the supplementary material). Thus, 3D reconstructions revealed that, at E13.5, ureteric branching defects in *Frs2α^UB–/–* kidneys were milder than in *Fgfr2^UB–/–*; however, there were no detectable differences between *Fgfr2/Frs2α^UB–/–* and *Fgfr2^UB–/–*. These findings could be consistent with Frs2α signaling downstream of Fgfr2, but clearly suggest that Fgfr2 signals through molecules other than Frs2α in the UB, including candidates such as phospholipase Cγ (PLCγ; Plcg1 – Mouse Genome Informatics), Crk2 (Cdk6 – Mouse Genome Informatics) and Src homology 2 domain-containing adapter protein B (Shb) (Eswarakumar et al., 2005; Lundin et al., 2003; Powers et al., 2000). Although all of the latter three molecules are expressed in kidney, PLCγ is a strong candidate for transmitting Fgfr2 signaling in the UB because mice chimeric for *PLCγ1^–/–* and wild-type cells develop severe renal dysplasia (Prosser et al., 2003; Shirane et al., 2001; Welsh et al., 1994).

At later stages, *Fgfr2/Frs2α^UB–/–* kidneys are more severely affected than either *Fgfr2^UB–/–* or *Frs2α^UB–/–* kidneys

At E17.5, although embryo sizes were comparable among all genotypes (not shown), both *Frs2α^UB–/–* and *Fgfr2^UB–/–* had smaller kidneys than controls by long axis and cross-sectional area (Fig. 3; see Table S4 in the supplementary material). However, *Fgfr2/Frs2α^UB–/–* mutants had dramatically smaller kidneys than any other genotype (including *Fgfr2^UB–/–*). Whole-mount calbindin immunostaining demonstrated that, compared with controls, *Frs2α^UB–/–* mice had relatively normal ureteric tip shapes, although there were slightly larger distances between tips (Fig. 3). *Fgfr2^UB–/–* kidneys had ureteric tips with aberrant shapes and longer distances between tips than kidneys of *Frs2α^UB–/–* mice (Fig. 3). *Fgfr2/Frs2α^UB–/–* mice, however, had more severe defects than all other genotypes with large regions devoid of tips (Fig. 3). E17.5 histological sections revealed that *Fgfr2/Frs2α^UB–/–* kidneys were disorganized with regions of outer cortex that were thin near areas of tubular dilatation (Fig. 3). Immunostaining for aquaporin 2 also showed that compound mutants had fewer collecting ducts than controls (Fig. 3).
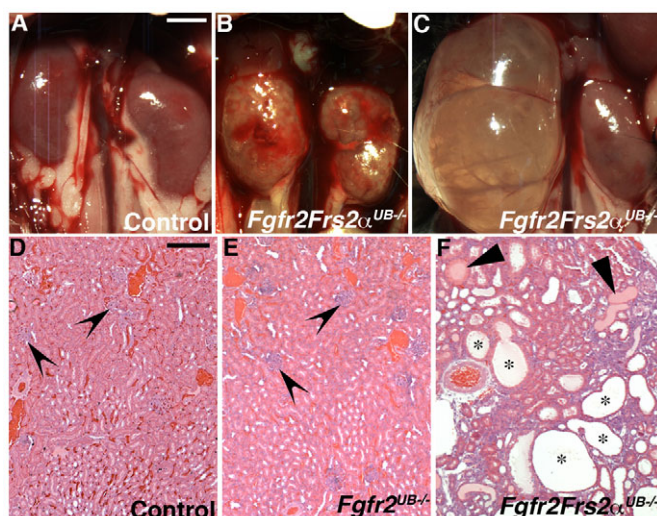
Fig. 4. P30 control and *Fgfr2/Frs2α^{UB–/–}* kidneys in situ hybridization and histological sections. (**A-C**) Compared with controls (A), *Fgfr2/Frs2α^{UB–/–}* mutants often have a translucent or cystic appearance (B) or frank hydronephrosis (C). (**D-F**) Compared with controls (D), *Fgfr2 ^{UB–/–}* kidneys (E) appear similar except that the glomeruli (concave arrowheads) are larger. By contrast, *Fgfr2/Frs2α^{UB–/–}* kidneys (F) are dysplastic with many cysts (asterisks) and have tubules filled with proteinaceous material (arrowheads). Scale bar: 0.25 cm for A-C; 150 μm for D-F.

By post-natal day 30 (P30), *Fgfr2/Frs2α^{UB–/–}* kidneys were significantly abnormal appearing translucent/cystic or frankly hydronephrotic (Fig. 4). Histological sections revealed that mutant kidneys had cystic dysplasia with tubular atrophy and proteinaceous casts (Fig. 4). Although some *Fgfr2^{UB–/–}* kidneys developed hydronephrosis (not shown), the parenchyma of these mutants had a relatively normal appearance (Fig. 4). Whereas *Frs2α^{UB–/–}* and *Fgfr2^{UB–/–}* glomeruli were larger than controls (by cross-sectional area and perimeter), *Fgfr2/Frs2α^{UB–/–}* glomeruli were larger than all other genotypes (see Fig. S2 in the supplementary material). Thus, beyond E13.5, *Fgfr2/Frs2α^{UB–/–}* had more severe kidney defects than all other genotypes. These findings strongly suggest additive roles for *Frs2α* and *Fgfr2* in the UB. The divergence in *Fgfr2^{UB–/–}* and *Fgfr2/Frs2α^{UB–/–}* renal abnormalities at later stages could still be consistent with Frs2α transmitting Fgfr2 signaling; however, it is possible that at early stages of ureteric and kidney morphogenesis, our assays were not sensitive enough to detect differences and that the two molecules signal independently.

Fgfr1^{UB–/–}Fgfr2^{LR/LR} kidneys are phenotypically normal

Fgfr2^{LR/LR} mice with point mutations in the Frs2α binding site on Fgfr2 had normal kidneys, suggesting independent roles of Fgfr2 and Frs2α in the UB (Sims-Lucas et al., 2009b). Although *Fgfr1* is present at low levels in the ureteric epithelium (as opposed to *Fgfr2*), wild-type Fgfr1 could form heterodimers with mutant Fgfr2, thus recruiting Frs2α (Poladia et al., 2006; Zhao et al., 2004). To avoid potential rescue by Fgfr1, mice were generated with conditional UB deletion of *Fgfr1* and with *Fgfr2^{LR/LR}* point mutations. E15.5 *Fgfr1^{UB–/–}Fgfr2^{LR/LR}* mice had normal ureteric branching by whole mount *Ret* in situ hybridization (see Fig. S3 in

the supplementary material). E17.5 *Fgfr1^{UB–/–}Fgfr2^{LR/LR}* kidneys had normal histology and size (see Fig. S3 and Table S5 in the supplementary material). Thus, blockade of Fgfr2 signaling through Frs2α in the UB does not affect kidney development, even with loss of Fgfr1. Wild-type Fgfr3 and/or Fgfr4 could also hypothetically form heterodimers with Fgfr2^{LR} and rescue kidney abnormalities; however, these receptors are also expressed at low levels in UB like *Fgfr1* (www.eurexpress.org/ee/). Thus, the most likely explanation is that Fgfr2 and Frs2α act independently in the UB.

Despite the presence of normal kidneys in *Fgfr1^{UB–/–}Fgfr2^{LR/LR}*, *Frs2α^{UB–/–}* mice have aberrant ureteric branching; thus, other RTKs must utilize Frs2α in the UB. Candidate RTKs with docking sites for Frs2α are Ret, neurotrophin receptors (Trks) and anaplastic lymphoma kinase (Alk). Ret is co-expressed with Frs2α in ureteric tips from E12.5 onward (unlike Fgfr2, which is expressed throughout the UB) (Hains et al., 2008; Pachnis et al., 1993; Sims-Lucas et al., 2009b; Zhao et al., 2004); furthermore, mice with point mutations in the Ret docking site for Frs2α (and other adapter proteins) have renal hypoplasia, similar to *Frs2α^{UB–/–}* mice (Jijiwa et al., 2004). Among Trks (Alpers et al., 1993; Durbeej et al., 1993; Wheeler et al., 1998), only *TrkB^{–/–}* mice have renal abnormalities in the juxtaglomerular apparatus (Garcia-Suarez et al., 2006). Kidneys of *Alk^{–/–}* mice have a normal appearance.

Conclusion

Although Fgfr2 and Frs2α have crucial roles in regulating UB morphogenesis, they appear to act in an independent and additive manner.

Competing interests statement
The authors declare no competing financial interests.

Supplementary material
Supplementary material for this article is available at
http://dev.biologists.org/lookup/suppl/doi:10.1242/dev.062158/-/DC1

References
Alpers, C. E., Hudkins, K. L., Ferguson, M., Johnson, R. J., Schatteman, G. C. and Bothwell, M. (1993). Nerve growth factor receptor expression in fetal, mature, and diseased human kidneys. *Lab. Invest.* **69**, 703-713.
Barasch, J., Qiao, J., McWilliams, G., Chen, D., Oliver, J. A. and Herzlinger, D. (1997). Ureteric bud cells secrete multiple factors, including bFGF, which rescue renal progenitors from apoptosis. *Am. J. Physiol.* **273**, F757-F767.
Barasch, J., Yang, J., Ware, C. B., Taga, T., Yoshida, K., Erdjument-Bromage, H., Tempst, P., Parravicini, E., Malach, S., Aranoff, T. et al. (1999). Mesenchymal to epithelial conversion in rat metanephros is induced by LIF. *Cell* **99**, 377-386.
Celli, G., LaRochelle, W. J., Mackem, S., Sharp, R. and Merlino, G. (1998). Soluble dominant-negative receptor uncovers essential roles for fibroblast growth factors in multi-organ induction and patterning. *EMBO J.* **17**, 1642-1655.
Costantini, F. and Kopan, R. (2010). Patterning a complex organ: branching morphogenesis and nephron segmentation in kidney development. *Dev. Cell* **18**, 698-712.
Durbeej, M., Soderstrom, S., Ebendal, T., Birchmeier, C. and Ekblom, P. (1993). Differential expression of neurotrophin receptors during renal development. *Development* **119**, 977-989.
Eswarakumar, V. P., Lax, I. and Schlessinger, J. (2005). Cellular signaling by fibroblast growth factor receptors. *Cytokine Growth Factor Rev.* **16**, 139-149.
Eswarakumar, V. P., Ozcan, F., Lew, E. D., Bae, J. H., Tome, F., Booth, C. J., Adams, D. J., Lax, I. and Schlessinger, J. (2006). Attenuation of signaling pathways stimulated by pathologically activated FGF-receptor 2 mutants prevents craniosynostosis. *Proc. Natl. Acad. Sci. USA* **103**, 18603-18608.

Garcia-Suarez, O., Gonzalez-Martinez, T., Germana, A., Monjil, D. F., Torrecilla, J. R., Laura, R., Silos-Santiago, I., Guate, J. L. and Vega, J. A. (2006). Expression of TrkB in the murine kidney. *Microsc. Res. Tech.* **69**, 1014-1020.

Gotoh, N. (2008). Regulation of growth factor signaling by FRS2 family docking/scaffold adaptor proteins. *Cancer Sci.* **99**, 1319-1325.

Hadari, Y. R., Gotoh, N., Kouhara, H., Lax, I. and Schlessinger, J. (2001). Critical role for the docking-protein FRS2 alpha in FGF receptor-mediated signal transduction pathways. *Proc. Natl. Acad. Sci. USA* **98**, 8578-8583.

Hains, D., Sims-Lucas, S., Kish, K., Saha, M., McHugh, K. and Bates, C. M. (2008). Role of fibroblast growth factor receptor 2 in kidney mesenchyme. *Pediatr. Res.* **64**, 592-598.

Jijiwa, M., Fukuda, T., Kawai, K., Nakamura, A., Kurokawa, K., Murakumo, Y., Ichihara, M. and Takahashi, M. (2004). A targeting mutation of tyrosine 1062 in Ret causes a marked decrease of enteric neurons and renal hypoplasia. *Mol. Cell. Biol.* **24**, 8026-8036.

Li, Z., Jerebtsova, M., Liu, X. H., Tang, P. and Ray, P. E. (2006). Novel cystogenic role of basic fibroblast growth factor in developing rodent kidneys. *Am. J. Physiol. Renal Physiol.* **291**, 289-296.

Lin, Y., Zhang, J., Zhang, Y. and Wang, F. (2007). Generation of an Frs2alpha conditional null allele. *Genesis* **45**, 554-559.

Lundin, L., Ronnstrand, L., Cross, M., Hellberg, C., Lindahl, U. and Claesson-Welsh, L. (2003). Differential tyrosine phosphorylation of fibroblast growth factor (FGF) receptor-1 and receptor proximal signal transduction in response to FGF-2 and heparin. *Exp. Cell Res.* **287**, 190-198.

Nguyen, H. Q., Danilenko, D. M., Bucay, N., DeRose, M. L., Van, G. Y., Thomason, A. and Simonet, W. S. (1996). Expression of keratinocyte growth factor in embryonic liver of transgenic mice causes changes in epithelial growth and differentiation resulting in polycystic kidneys and other organ malformations. *Oncogene* **12**, 2109-2119.

Ohuchi, H., Hori, Y., Yamasaki, M., Harada, H., Sekine, K., Kato, S. and Itoh, N. (2000). FGF10 acts as a major ligand for FGF receptor 2 IIIb in mouse multi-organ development. *Biochem. Biophys. Res. Commun.* **277**, 643-649.

Pachnis, V., Mankoo, B. and Costantini, F. (1993). Expression of the c-ret proto-oncogene during mouse embryogenesis. *Development* **119**, 1005-1017.

Perantoni, A. O., Dove, L. F. and Karavanova, I. (1995). Basic fibroblast growth factor can mediate the early inductive events in renal development. *Proc. Natl. Acad. Sci. USA* **92**, 4696-4700.

Poladia, D. P., Kish, K., Kutay, B., Hains, D., Kegg, H., Zhao, H. and Bates, C. M. (2006). Role of fibroblast growth factor receptors 1 and 2 in the metanephric mesenchyme. *Dev. Biol.* **291**, 325-339.

Powers, C. J., McLeskey, S. W. and Wellstein, A. (2000). Fibroblast growth factors, their receptors and signaling. *Endocr. Relat. Cancer* **7**, 165-197.

Prosser, S., Sorokina, E., Pratt, P. and Sorokin, A. (2003). CrkIII: a novel and biologically distinct member of the Crk family of adaptor proteins. *Oncogene* **22**, 4799-4806.

Qiao, J., Uzzo, R., Obara-Ishihara, T., Degenstein, L., Fuchs, E. and Herzlinger, D. (1999). FGF-7 modulates ureteric bud growth and nephron number in the developing kidney. *Development* **126**, 547-554.

Qiao, J., Bush, K. T., Steer, D. L., Stuart, R. O., Sakurai, H., Wachsman, W. and Nigam, S. K. (2001). Multiple fibroblast growth factors support growth of the ureteric bud but have different effects on branching morphogenesis. *Mech. Dev.* **109**, 123-135.

Revest, J. M., Spencer-Dene, B., Kerr, K., De Moerlooze, L., Rosewell, I. and Dickson, C. (2001). Fibroblast growth factor receptor 2-IIIb acts upstream of Shh and Fgf4 and is required for limb bud maintenance but not for the induction of Fgf8, Fgf10, Msx1, or Bmp4. *Dev. Biol.* **231**, 47-62.

Schuchardt, A., D'Agati, V., Larsson-Blomberg, L., Costantini, F. and Pachnis, V. (1994). Defects in the kidney and enteric nervous system of mice lacking the tyrosine kinase receptor Ret [see comments]. *Nature* **367**, 380-383.

Shirane, M., Sawa, H., Kobayashi, Y., Nakano, T., Kitajima, K., Shinkai, Y., Nagashima, K. and Negishi, I. (2001). Deficiency of phospholipase C-gamma1 impairs renal development and hematopoiesis. *Development* **128**, 5173-5180.

Sims-Lucas, S., Argyropoulos, C., Kish, K., McHugh, K., Bertram, J. F., Quigley, R. and Bates, C. M. (2009a). Three-dimensional imaging reveals ureteric and mesenchymal defects in Fgfr2-mutant kidneys. *J. Am. Soc. Nephrol.* **20**, 2525-2533.

Sims-Lucas, S., Cullen-McEwen, L., Eswarakumar, V. P., Hains, D., Kish, K., Becknell, B., Zhang, J., Bertram, J. F., Wang, F. and Bates, C. M. (2009b). Deletion of Frs2alpha from the ureteric epithelium causes renal hypoplasia. *Am. J. Physiol. Renal Physiol.* **297**, F1208-F1219.

Welsh, M., Mares, J., Karlsson, T., Lavergne, C., Breant, B. and Claesson-Welsh, L. (1994). Shb is a ubiquitously expressed Src homology 2 protein. *Oncogene* **9**, 19-27.

Wheeler, E., Gong, H., Grimes, R., Benoit, D. and Vazquez, L. (1998). p75NTR and Trk receptors are expressed in reciprocal patterns in a wide variety of non-neural tissues during rat embryonic development, indicating independent receptor functions. *J. Comp. Neurol.* **391**, 407-428.

Yu, K., Xu, J., Liu, Z., Sosic, D., Shao, J., Olson, E. N., Towler, D. A. and Ornitz, D. M. (2003). Conditional inactivation of FGF receptor 2 reveals an essential role for FGF signaling in the regulation of osteoblast function and bone growth. *Development* **130**, 3063-3074.

Zhao, H., Kegg, H., Grady, S., Truong, H. T., Robinson, M. L., Baum, M. and Bates, C. M. (2004). Role of fibroblast growth factor receptors 1 and 2 in the ureteric bud. *Dev. Biol.* **276**, 403-415.